Acceleration of microiron-based dechlorination in water by contact with fibrous activated carbon

*Maria Vogel, Frank-Dieter Kopinke, Katrin Mackenzie**

Helmholtz Centre for Environmental Research – UFZ, Department of Environmental Engineering, D-04318 Leipzig, Germany

* Corresponding author e-mail: katrin.mackenzie@ufz.de

Abstract

Zero-valent iron (ZVI) is widely applied for reduction of chlorohydrocarbons in water. Since the dechlorination occurs at the iron surface, marked differences in rate constants are commonly found for nanoscale and microscale ZVI. It has already been shown for trichloroethene (TCE) adsorbed to activated carbon (AC) that the dechlorination reaction is shifted to the carbon surface simply by contacting the AC with highly reactive nanoscale ZVI particles. Transfer of reactive species to the adsorbed pollutant was discussed.

The present study shows that even low price and very low reactive microscale ZVI can also be utilized for an effective dechlorination process. Compared to the reaction rate at the iron surface itself, an enormous acceleration of the dechlorination rate for chlorinated ethenes was observed, reaching activity levels such as known for nanoscale ZVI. When fibrous AC is brought into direct contact with microscale ZVI the iron-surface-normalised dechlorination rate constants increased by up to four orders of magnitude. This implies that the dechlorination

reaction is fully transferred to the AC surface. At the same time, the anaerobic corrosion of the same material was not substantially affected. Thus, the utilization of iron's reduction equivalents towards dechlorination (dechlorination efficiency) can be considerably enhanced. A screening with various AC types showed that the extent of rate acceleration depends strongly on the surface chemistry of the AC. By means of temperature-programmed desorption, it could be shown that concentration and type of oxygen surface groups determine the redox-mediation properties. Quinone/hydroquinone groups were identified as being the main drivers for electron-transfer processes, but to some extent other redox-active groups such as chromene and pyrone can also act as redox mediators. AC overall plays the role of a catalyst rather than a reactant. The present study derives recommendations for practical application of the findings in water-treatment approaches.

Keywords: dechlorination in the adsorbed state, zerovalent iron, activated carbon, redox mediator

1. Introduction

In the last 20 years, application of ZVI has become the method of choice for *in-situ* and on-site reduction of chlorinated hydrocarbons in aquifers [1,2]. Microscale ZVI (mZVI) and granular iron filings have found application in classical permeable reactive barriers, whereas the more reactive injectable, but cost-intensive, nanoscale ZVI has gained attention in research and field application for *in-situ* installation of reaction zones [3]. However, one remaining restriction for

all pristine iron particles is the low affinity of hydrophobic contaminants to the metal surface, which limits the performance of remediation, particularly at low contaminant concentrations [4–8]. One way to overcome this issue is the combination of ZVI with sorption-active carriers, such as activated carbon (AC), forming composite materials [9–18] which allow the sorptive enrichment of organic pollutants in the vicinity of the reactive iron centres, and therefore lead to a more efficient iron utilisation for the target reaction [13]. It is noteworthy that the contaminant degradation in such composites takes place even though the reactive metal surface and the adsorption site for contaminants are spatially separated [14]. Recent studies showed that even in systems with separated AC and nanoscale ZVI particles, which only collide from time to time in an agitated aqueous slurry, a degradation of chlorinated ethenes takes place [19,20]. This raises two questions: (i) how does the transfer of reactive species from their site of origin to the site of contaminant degradation occur, and (ii) what is the role of the carbonaceous sorbent surface.

Generally, carbon materials are known to take an active part in chemical reactions by allowing electron transfer and possibly also hydrogen spill-over [19–22]. It has been found that reaction rates of reductive transformations can be increased, e.g. the reduction of nitroaromatics in the presence of sulfide [23–26] or ZVI [22,27] as reductants. AC is also able to enhance the hydrolysis of 1,1,2,2-tetrachloroethane [28,29] or γ-hexachlorocyclohexane [30]. Furthermore, the microbial degradation of organic contaminants can be mediated and accelerated in the presence of AC [31–33]. Thereby, structural elements, e.g. defect sites of graphitic hexagonal crystallites, unsaturated valences at break lines and edges, and the presence of heteroatoms or different functional groups are discussed and presumed to play a decisive role [21]. However, it

was also found that carbonaceous materials have the potential to inhibit chemical reactions at iron metal [5,8]. Graphitic structures at the surface of cast-iron particles can lead to non-reactive sorption. Consequently, the combination of carbonaceous materials with ZVI offers on the one hand the chance for efficient contaminant degradation but on the other hand can also increase the risk of contaminant protection.

The objective of the present study is a closer examination of the mZVI-based dechlorination of typical groundwater contaminants, such as trichloroethene (TCE) and tetrachloroethene (PCE) in the presence of AC with regard to economic optimization. mZVI was chosen for the study instead of nanoscale ZVI as there is a strong gap between the low price on the one hand and the insufficient reactivity towards pollutants on the other hand, due to its low specific surface area (about 0.1-1 m^2 g^{-1}). If this gap could be reduced, the attractiveness of mZVI for practical application in any water treatment approach would be much higher. The present study will examine the combination of AC and mZVI in batch experiments, where various types of AC textiles will be applied in tight contact with mZVI particles in order to ensure a physical contact between the two materials. The role of the textile AC materials for their abilities to influence the dechlorination reaction will be discussed and brought into relation to their surface structural properties with the main emphasis put on oxygen-containing functional groups. In addition, the iron consumption by dechlorination and by the competing anaerobic corrosion, i.e. the progressive loss of reduction equivalents due to the reaction of iron with water, will support the discussion.

2. Experimental section

2.1. Materials

High-purity carbonyl-based mZVI particles ($d_p \approx 10$ µm, $A_{BET} \approx 0.2$ m² g^{-1}, $x_{Fe(0)} \geq 99$ wt-%), $NaHCO_3$ (analytical grade) and HNO_3 (65 %) were purchased from Merck, Germany. AC textiles were obtained from Actitex, France. The fibrous AC materials are manufactured from synthetic viscose substrates and processed as cloth and felts. Their physical and chemical properties are listed in Table 1. Ultrapure water (Millipore Simplicity 185, 18.2 MΩ cm) was used for the preparation of the reaction media of all batch experiments. PCE (99 %) and TCE (99 %) were obtained from Sigma Aldrich, Germany, and directly used without further purification. Methanol (99.7 %) was obtained from Chemsolute, Germany.

Table 1: Physical and chemical properties of studied AC textiles.

Sample	Layer thickness	Weight per layer surface	BET surface area*	Total pore volume*	Mean pore diameter*	pH at point of zero charge
	[mm]	[g m^{-2}]	[m^2 g^{-1}]	[cm^3 g^{-1}]	[nm]	
FC 10	3	260	1400	0.7	1.9	6.6
FC 15	2	110	1400	0.7	1.9	7.3
FC 12	2.5	140	1100	0.5	1.7	4.6
WKL 20	0.4	100	1100	0.5	1.9	5.9
RS 13	0.5	220	1000	0.5	1.8	7.2
VS 19	0.6	145	2100	1.0	1.8	7.3

* derived from Brunauer-Emmett-Teller (BET) adsorption/desorption isotherms (N_2 at 77 K)

2.2. Analytical methods

The quantitative analysis of chlorine-free C_2-products (acetylene, ethylene and ethane) and the semi-quantitative analysis of C_3- and C_4-coupling products were performed by means of headspace sampling and GC-FID analysis (GC-2010 plus, Shimadzu Corp. equipped with a GS-Q Plot column from Agilent). The analysis of chloride generated during dechlorination was performed by means of ion chromatography (IC 25, Dionex equipped with an IonPacAS15/AG15). The concentrations of the halogenated substances PCE, TCE, dichloroethenes (DCEs) and vinyl chloride (VC) were monitored during the batch experiments by means of headspace sampling and GC-MS analysis (GC-MS-QP2010, Shimadzu, equipped with a HP5 capillary column) taking into account the underlying distribution and sorption equilibria. In order to analyse the chlorinated ethenes, which were adsorbed at the textile AC, solvent extraction using a hexane-propanol mixture (1 : 1, 16 h) with toluene as internal standard was performed, followed by GC-MS analysis of the extracts.

The anaerobic corrosion of mZVI according to the equation $Fe^0 + 2\ H_2O \rightarrow Fe^{2+} + H_2 + 2\ OH^-$ was monitored by measuring the hydrogen concentration in the headspace volume over suspended particles (with methane as internal standard, allowing extension of the headspace in order to avoid overpressure) using a GC-TCD (HP6850, HP PLOT column).

Temperature-programmed desorption (TPD) of AC samples was performed using a BELCAT-B chemisorption analyser (BEL Japan, Osaka) connected with a mass spectrometer (MKS Cirrus 2). Released gases such as carbon monoxide and dioxide (CO and CO_2) were transferred via a direct-coupling capillary and measured by analysis of their MS signal. The samples were first

pre-treated at 150 °C for 30 min in an argon atmosphere. They were then heated up from 150 °C to 1100 °C in a helium flow (50 mL min^{-1}) with a heating rate of 10 K min^{-1}.

The point of zero charge (PZC) of the textile AC samples was determined according to Babic et al. by means of the immersion method. [34].

2.3. Dechlorination studies

The dechlorination experiments with mZVI alone and mZVI in combination with textile AC were performed according to the following procedure: 50 mL of a 5 mM $NaHCO_3$ solution (pH ≈ 8.5) was added to a 120 mL crimped serum bottle and purged with argon. A defined amount of mZVI was placed inside a hand-sewed pouch of textile AC, which was closed and added to the bottle (Figure 1). The pouch varied in its size depending on the applied mass of AC and ranged between 1-3 cm^2 cross-section areas. In all cases, a tight physical contact between the iron particles and the AC felt was ensured. After further purging with argon, the bottles were closed airtight using aluminium crimp caps with PTFE-lined septa and treated for 10 min in an ultrasonic bath. A defined volume of methane was added as internal standard.

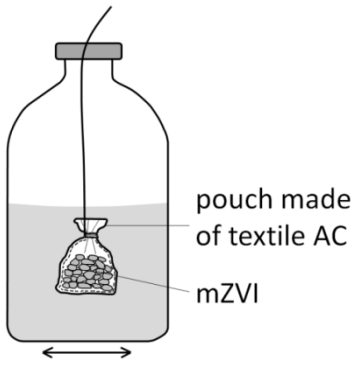

Figure 1: Scheme of the experimental arrangement

The reaction was started by injecting a methanolic stock solution of PCE or TCE. The bottles were continuously shaken at room temperature on a horizontal shaker at 90 rpm. The agitation intensity effected a fast mixing of the aqueous phase around the suspended mZVI particles or the AC pouches, whereas the mZVI bed inside the pouches remained largely unaffected ('static'). In order to test the longevity of the catalytic activity of the AC felt FC 10, the batch was prepared as described above, whereby the mZVI-filled AC pouch was pre-conditioned in the argon-purged 5 mM $NaHCO_3$ solution for three days before TCE was added. After one week of reaction time, the bottle was purged with argon and fresh TCE was re-spiked. This procedure was repeated three times.

2.4. Pre-treatment of the carbon felt FC 10

A sample of the AC felt FC 10 (3 g L^{-1}) was pre-treated with mZVI (60 g L^{-1}) for four days in argon-purged 5 mM $NaHCO_3$ aqueous suspension. In order to achieve this, iron particles were placed in a closed AC pouch and slightly shaken as described above. After this conditioning time, the iron particles were removed from the carbon felt and several washing steps with argon-purged, deionised water were performed. The treated AC sample was dried for 45 min at 105 °C under nitrogen atmosphere and analysed by means of TPD analysis.

Furthermore, the surface of the AC felt FC 10 was modified in two ways: (i) by wet oxidation using nitric acid. 1 g of AC was oxidised with 100 mL 5 M HNO_3 under reflux at 90 °C for 24 h. Subsequently, the felt was washed several times with deionised water and dried at 110 °C overnight. (ii) The AC felt FC 10 was heated up to 1100 °C under an inert He-atmosphere and re-

exposed to air after cooling. Thereby most of the functional surface groups were removed, however, the re-formation of a small amount of new O-functionalised groups was possible [35].

3. Results and discussion

3.1. Dechlorination of TCE and PCE by mZVI

TCE and PCE were chosen as typical groundwater contaminants for which adsorption to AC is one of the treatment options but which are also subject to chemical reduction by metallic iron in aqueous media. Both substances show very similar dechlorination behaviour with iron and are therefore chosen comparably in this study. Dechlorination of both substances with mZVI was examined in benchmark experiments. The mZVI under study is a very slow-reacting, high-purity iron which was chosen in order to avoid any effects of trace-level catalytically active metals and carbon impurities. Pre-treatment of mZVI by washing with diluted acids appeared to have no marked influence on either dechlorination or corrosion rates and thus was omitted. In duplicate tests, the dechlorination kinetics for TCE and PCE were monitored by means of chlorine-free C_2-hydrocarbons and chloride analysis over a time period of 400 h. For both model contaminants, ethylene and ethane formation was prevalent, whereas acetylene was found only in traces with pure iron as reductant. Partially chlorinated products were formed only in trace amounts, and are not discussed further here. First-order rate constants (k_{obs}) for dechlorination with iron were calculated from the disappearance of chloroethenes and the appearance of products. For TCE and PCE dechlorination, $k_{obs,TCE} = 2.6 \cdot 10^{-4}\ h^{-1}$ and $k_{obs,PCE} = 2.0 \cdot 10^{-4}\ h^{-1}$, respectively, were found (reaction conditions applied: $c_{0,TCE} = 20\ mg\ L^{-1}$ or $c_{0,PCE} = 25\ mg\ L^{-1}$, $c_{mZVI} = 400\ g\ L^{-1}$, 5 mM $NaHCO_3$, $pH_{start} = 8.4$). The reaction selectivity towards the sum of ethylene

and ethane formation was roughly constant over the duration of the experiments ($n_{ethylene}$: n_{ethane} ≈ 1 : 1). The yields of C_2-hydrocarbons during the reaction were similar: 62 % and 56 % for TCE and PCE, respectively. As commonly performed, the iron-surface normalised (second order) rate constants (k_{SA}) were calculated as the descriptor for the dechlorination activity of ZVI. The obtained values $k_{SA,TCE} = 3.25 \cdot 10^{-6}$ L m^{-2} h^{-1} and $k_{SA,PCE} = 2.5 \cdot 10^{-6}$ L m^{-2} h^{-1} are in the lower range of k_{SA} values cited in the literature for various iron materials, but are in the same order of magnitude as known for other iron samples of high purity grade [36–38] .

3.2. PCE dechlorination in the mZVI+AC system - test of various textile AC types

In contrast to the experiments described in the literature, where AC particles and nanoscale ZVI were brought into loose non-continuous contact [19,20], the textile AC pouches used in the present study allow continuous physical contact between the enclosed mZVI and the AC. The entire system was slightly shaken in order to ensure mass transport and to avoid stationary hydrogen bubbles at the AC pouches. Thus, transport of reactive species is facilitated from the surface of the iron particles to the target compound, which is predominantly located at the internal AC surface [19,20]. After the addition of PCE to the reaction vessel, the major part of the contaminant was rapidly adsorbed by the textile AC. Within 24 h, an equilibrium state was approached with an adsorbed fraction of > 99.9 %, such that the share of the reaction of freely dissolved PCE with the iron particles can be considered negligible. In order to exclude any influence of different specific surface areas of the AC textiles on the dechlorination, the offered carbon surface area concentration was kept constant for all batches ($c_{SA,AC}$ = 1800 m² L^{-1}), thus the textile sheet size was adjusted accordingly. The dechlorination progress was monitored by

means of headspace analysis of chlorine-free C_2-products, which were, in contrast to the chlorinated educts, not significantly affected by sorption to the AC surface.

Results for PCE degradation in the mZVI+AC system are shown in Figure 2. Although significantly lower amounts of mZVI were applied in the AC pouches (c_{mZVI} = 7 g L^{-1}) compared to the benchmark experiment without AC (c_{mZVI} = 400 g L^{-1}), an accelerated dechlorination of PCE was observed in the presence of four out of the six investigated AC textile samples. The corresponding PCE conversion with the low iron concentration (c_{mZVI} = 7 g L^{-1}) in absence of AC (not shown in Figure 2) amounted to only 0.1 % after 400 h.

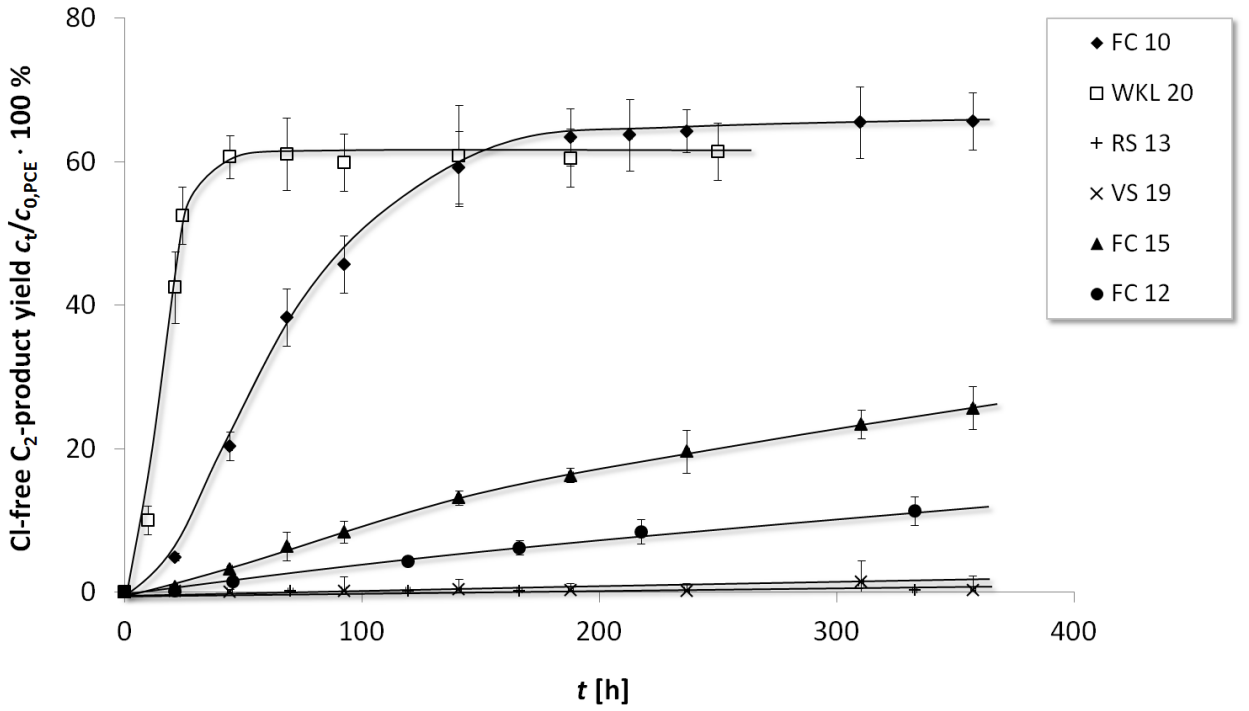

Figure 2: Kinetics of the PCE dechlorination in the presence of mZVI and various activated carbon textiles ($c_{0,PCE,total}$ = 12.5 mg L^{-1}, c_{mZVI} = 7 g L^{-1}, c_{AC} = 1-2 g L^{-1}, c_{NaHCO3} = 5 mM, pH_{start} = 8.4). The error bar represents the mean deviation of single values from the mean value with n = 3 to 5.

This result is markedly different from published data regarding particle-particle contact between nanoscale ZVI and AC [19,20], where the AC did decrease the TCE reaction rate. AC can be seen as an adsorption sink for the TCE, which thus is withdrawn from the reactive nanoiron surface. Nevertheless, the authors could show that the dechlorination reaction occurred predominantly at the AC surface. The transfer of reactive species from the iron to the AC surface was, however, slower than the TCE reduction at the bare metal. Differing from these literature findings, in the present study slowly reacting metal particles were applied. We experience for some AC types a strong acceleration of the dechlorination reaction in the mixed particle suspension compared with the bare metal suspension without AC. Presence of other AC types (e.g. RS 13, VS 19 in Fig. 2) showed only a minor effect. This emphasizes the role of the AC type for the performance of the ZVI+AC system.

In all cases the product selectivity for mZVI+AC was similar and was characterised by a prevailing acetylene formation. Typically, at PCE conversion degrees of about 10 % the C2 products consist of 80 % acetylene, 14 % ethylene and 6 % ethane (primary product selectivities). It has to be pointed out that the AC textiles WKL 20 and FC 10 supported the dechlorination to a higher extent, thus the maximum concentration of chlorine-free C_2-products was already reached after 50 and 200 h, respectively. The solvent extraction of these AC textiles after the reaction (t = 400 h) revealed that only traces of PCE were left, indicating a nearly complete conversion of the contaminant. As generally observed for ZVI as reducing agent of chloroethenes, also the present study showed product selectivities toward chlorine-free C_2-hydrocarbons of less than 100 %. We found a maximum of 65 % of the PCE taking this reaction pathway while 100 % C-Cl bond-breaking was observed (full conversion to chloride). That points to parallel reaction pathways

forming higher-molecular-weight dechlorinated products [49]. However, since the percentage of the headspace-observable formation to C_2 hydrocarbons varies only slightly, this reaction pathway is mostly used here for comparison of the various mZVI+AC systems.

The course of the chlorine-free C_2-product formation in the presence of mZVI in contact with the AC felt FC 10 followed a pseudo-first-order kinetics yielding $k_{obs,PCE} = 1.7 \cdot 10^{-2}\ h^{-1}$, which corresponds formally to an iron-surface-normalised rate constant of $k_{SA,PCE} = 1.2 \cdot 10^{-2}\ L\ m^{-2}\ h^{-1}$. This is a factor of 5000 faster than observed for the same mZVI in the absence of AC. For the AC cloth WKL 20, the acceleration effect is even higher by about one order of magnitude (i.e. a factor of 50,000). On the other hand, in the presence of the woven textile AC types RS 13 and VS 19, almost no PCE dechlorination activity was detected.

This raises the questions of how the large differences in the chemical activities of these AC textiles in the dechlorination reaction can be explained, and what the mechanism of the interplay between ZVI and AC is. It can be assumed that a multitude of properties of the AC play a role, whereby only a selection is discussed in the present study. The general 'physical' characterisation of the carbon types (see Table 1), including PZC and porosity parameters, did not reveal significant differences in properties which could be responsible for the different chemical behaviour of the AC textiles. Furthermore, the texture showed overlaps which would not explain the differences in chemical reaction behaviour. When we assume that the reaction site is shifted from the ZVI surface to the AC surface, the chemical composition of the AC surface is more likely to be of importance, e.g. the presence of various oxygen-containing functional groups [21]. Some of them are known to take an active part in chemical reactions, e.g. as redox mediators [21,26]. In order to obtain information about quantity and quality of these groups at

the surface of the various AC textiles, TPD analyses were performed. TPD has been used by several working groups to not only (indirectly) identify but also to quantify the various surface groups in carbon materials by release of carbon oxides at specific temperature ranges. The method has been applied in order to prove chemical changes in surface properties and to correlate chemical and catalytic properties of oxidized activated carbon [39-42].

The derived oxygen contents of the analysed carbon samples are shown in Table 2. The high oxygen contents of the two samples FC 10 and WKL 20 correlate with their high chemical activity in the ZVI-driven dechlorination experiments. In addition to the amount of the oxygen-containing functional groups, their type is expected to be relevant for participation in redox reactions. The functional groups present on the AC surface can be derived from the position of CO and CO_2 peaks in temperature-resolved TPD profiles (

Figure **3**).

Table 2: Oxygen content of activated carbon textiles (derived from TPD analysis).

	Oxygen content [wt-%]
FC 10	15.9
FC 15	3.9
FC 12	3.0
WKL 20	13.7
RS 13	5.2
VS 19	2.5

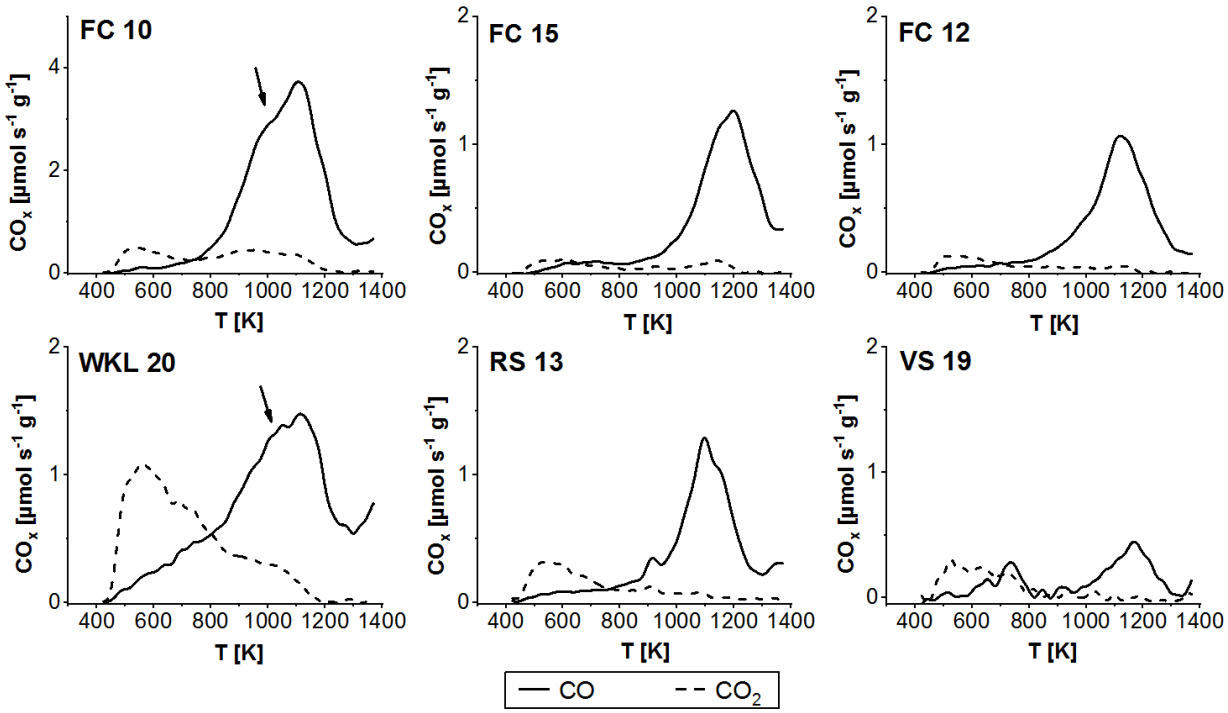

Figure 3: TPD profiles of activated-carbon textiles under study (heating rate 10 K min^{-1}). The dashed lines represent the release of CO_2, while the solid lines show CO elimination.

The release of CO_2 at about 500 K can be assigned to the decomposition of carboxylic groups. It occurred for all AC samples but to different extents. A correlation between the chemical activity of the AC types and the CO_2 release was not found. Another typical TPD peak at 1100 to 1200 K was also observed for all carbon types. It can be assigned to the destruction of carbonyl groups [39]. Also here, no correlation with the chemical activities is obvious. However, a marked difference between the carbon samples was observed for the release of CO apparent as a shoulder peak at about 1000 K (arrow), indicating phenolic groups [39]. The phenolic groups seem to be especially pronounced for the FC 10 and WKL 20 samples, but less notable for FC 12, FC 15, VS 19 and RS 13. This finding leads to the hypothesis that functional structures with

297 phenolic groups at the carbon surface are involved in the iron-driven dechlorination. It is
298 postulated that a special representative of phenolic groups, the hydroquinone group, acts
299 together with its oxidised quinone form as redox mediator, as is known from literature data for
300 other reduction processes [26,31,32]. In order to obtain further information about the
301 corresponding reaction mechanisms and the involvement of oxygen-containing functional
302 groups, the AC felt FC 10 was chosen for further investigation.
303
304 **3.3. Study of the mZVI+FC 10 system**
305
306 *3.3.1. TCE dechlorination with mZVI+FC 10*
307 Figure 4 shows results from a typical experiment with mZVI packed in pouches made of the AC
308 felt FC 10 for TCE degradation, whereby educt degradation and formation of all intermediates
309 and final products was monitored over more than five days. PCE and TCE react in a similar way,
310 but TCE was chose for this study in order to avoid overlaps in DCE and VC product formation.
311 The release of > 96 % of the theoretically expected chloride amount after 140 h indicates an
312 almost complete degradation of the contaminant. Compared to the benchmark experiment
313 without AC at c_{mZVI} = 400 g L^{-1}, in which roughly 4 % of the TCE was dechlorinated by mZVI alone,
314 an approximately 13-fold lower concentration of mZVI in the presence of AC leads to complete
315 TCE reduction within the same time period. After 140 h reaction time, TCE was converted to
316 62 % acetylene, 13 % ethene, 5 % ethane, > 7 % C_3- and C_4-coupling products and 2 % VC (all
317 data as mol-%). The detected products cover ≥ 90 % of the TCE C-balance. A balance gap
318 remained. Further coupling products were probably formed as known for reactions at Fe

surfaces [52] but not detected by headspace analysis. A final solvent extraction of the AC might deliver more information, but was not performed in this study because the main message of the present study is not affected.

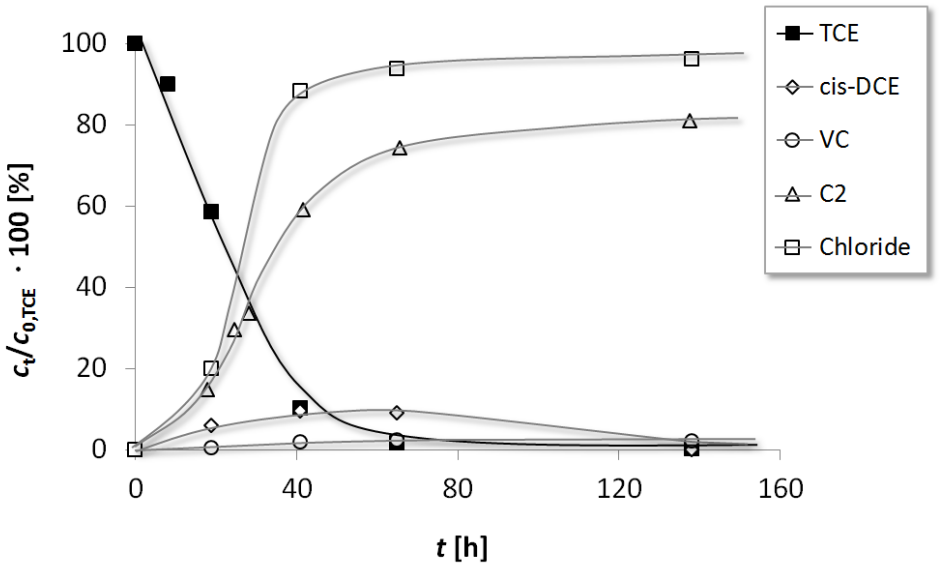

Figure 4: Kinetics of TCE dechlorination in the presence of mZVI and the activated carbon felt FC 10 ($c_{0,TCE,total}$ = 20 mg L^{-1}, c_{FC10} = 3.4 g L^{-1}, c_{mZVI} = 30 g L^{-1}, c_{NaHCO3} = 5 mM, pH_{start} = 8.4).

One of the plausible reaction pathways is a stepwise dechlorination, since DCEs (max. 10 %) and VC (max. 2.5 %) were detected as intermediates. They undergo further dechlorination and are therefore not regarded as dead-end products here. The appearance of partially dechlorinated intermediates and the dominance of acetylene as final product are indicators for a limitation of active hydrogen as reactive species [20]. In a former study, Kopinke et al. conducted an experiment using a carbon cathode for TCE reduction, which predominantly transferred electrons but no hydrogen species to AC-adsorbed TCE [19]. These conditions led to a similar product spectrum as found in this study for the mZVI+FC 10 system. However, when TCE was

degraded in the presence of freely suspended nanoscale ZVI and AC particles, the product spectrum was comparable to those found in systems containing exclusively nanoscale ZVI, indicating the participation of both electrons and active hydrogen in the dechlorination process. In the present study, a limitation in the availability of nascent hydrogen (H*) might occur during the fast dehalogenation, since the available iron surface was substantially smaller than in the study of Kopinke et al. [19]. Increase of ZVI-to-AC ratio leads to a higher hydrogenation degree. In addition to the availability of reactive species, the nature of attachment of chlorinated ethenes to the different material surfaces could also be responsible for any differences in the product spectrum. While TCE is chemisorbed to the iron surface, forming pi- and di-sigma-bonds [43], the interaction of the chlorinated ethenes to the AC is dominated by physisorption [44].

The reaction of TCE in the mZVI+FC 10 system is characterised by a lag phase during the first ten hours, showing a lower dechlorination rate. This phenomenon was not observed for mZVI alone. Hence, a conditioning of the AC surface is a more likely process than an activation of the iron surface. This raises the question of how the AC surface is modified during this initial reaction phase. In order to explain this phenomenon, the carbon felt FC 10 was pre-treated with mZVI in aqueous suspension and then analysed again by means of TPD. The resulting TPD profile is shown in Figure 7A. It clearly reveals the formation of additional groups releasing CO at about 1050 K, which can be ascribed to phenolic groups [39]. At the same time, a decrease of CO-releasing groups between 1100 and 1200 K was observed, which can be interpreted as a decline of carbonyl groups [39]. Based on these observations it can be assumed that during the contact time between mZVI and AC felt in aqueous environment, reduction of quinones to hydroquinone groups may occur at the AC surface, and that the hydroquinone groups in turn

358 are able to take part in reductive dechlorination of the adsorbed chloroethenes. The redox-
359 mediating properties of quinone derivatives in various reactions have been described in the
360 literature [45,46]. In addition, AC-surface-bound quinoid groups are able to support redox
361 reactions, as has been described not only for microbial processes [31,32], but also for the
362 chemical reduction of nitroaromatics with sulfide [26] and the reduction of congo red [47].
363
364 *3.3.2. Dependence of dechlorination rates on ZVI concentration*
365 When pure ZVI reacts with TCE in aqueous suspensions, the observed first-order rate coefficient
366 k_{obs} strictly depends on the applied ZVI concentration. The second-order surface-normalized
367 dechlorination kinetics is more-or-less a material property. A completely different picture is
368 obtained when ZVI is embedded in AC, forming a new composite material (such as Carbo-Iron),
369 with k_{obs} remaining roughly constant within a wide range of composite concentration [13]. In
370 the present study, various amounts of mZVI were embedded into pouches of the AC felt FC 10
371 and the resulting k_{obs} were compared. Figure 5 shows the formation of C_2-hydrocarbons over
372 time (A) and the corresponding first-order kinetics plots (B).
373 For all batch tests, a lag phase (discussed in 3.3.1) was observed at the beginning of the
374 reaction: it lasted up to about 30 hours and decreased with increasing iron concentration. After
375 the lag phase, the product formation followed first-order kinetics, as the resulting linear plots in
376 semi-logarithmic coordinates show. The various slopes of the regression lines, thus the
377 observed dechlorination rate coefficients $k_{obs,}$ were in the range of 0.037 h^{-1} to 0.047 h^{-1} for all
378 applied ZVI concentrations from 10 to 90 g L^{-1}.
379

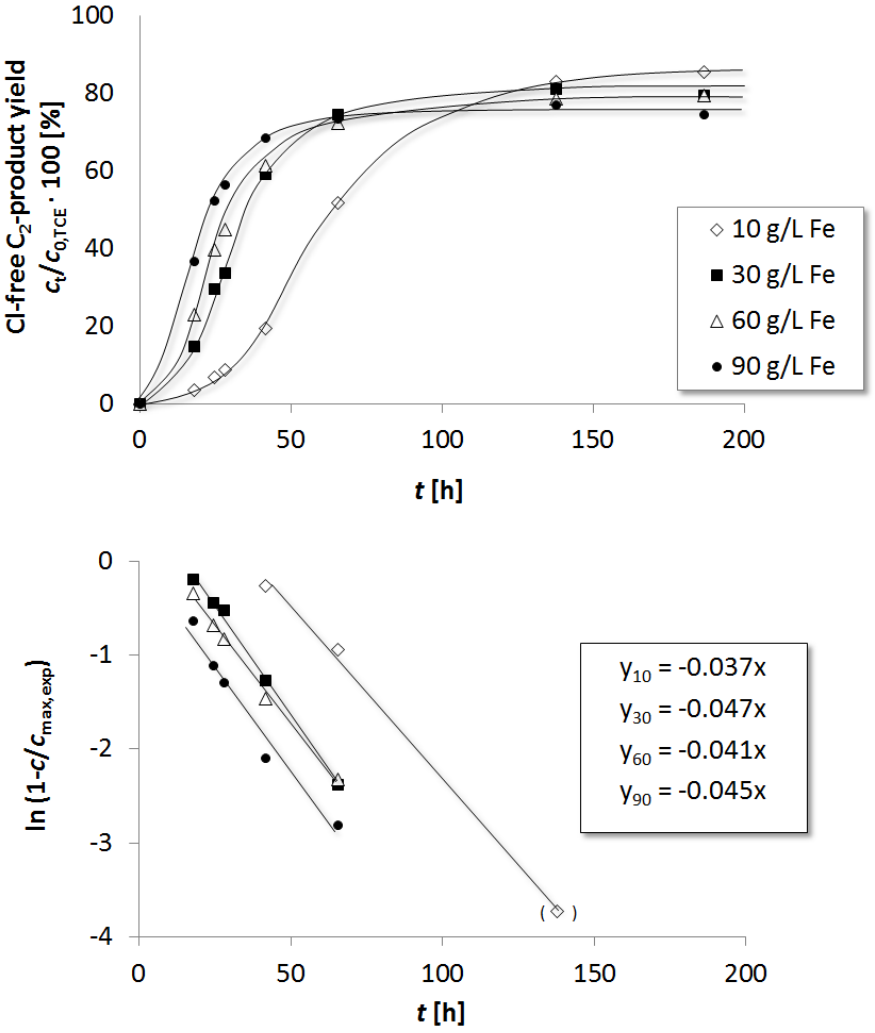

380

381 Figure 5: Kinetics of TCE reduction with various amounts of mZVI embedded into AC-felt
382 pouches. ($c_{0,TCE,total}$ = 20 mg L^{-1}, $c_{Fe(0)}$ = 10 to 90 g L^{-1}, AC: FC 10, $c_{FC\ 10}$ = 3.4 g L^{-1}, c_{NaHCO3}
383 = 5 mM, pH_{start} = 8.4).
384

385

386 This means that the observed TCE dechlorination rates did not depend on the applied iron
387 concentrations under the applied conditions. This can be explained by the fact that the reaction
388 takes place at the carbon surface, where the supply of reactive species (most likely electrons)
389 from the iron particles is not rate-limiting above a certain contact level between ZVI and fibrous
390 AC.

391 The phenomenon appears similar to dechlorination kinetics with Carbo-Iron, where the reaction
392 rate was also observed to be largely independent of its concentration [13]. However, the
393 mechanistic background may be different in the two systems. As discussed already for Carbo-
394 Iron, the different reaction kinetics make a direct comparison of second-order rate coefficients
395 between carbon-containing and carbon-free ZVI-based systems difficult [13].
396 While for the activity of different ZVI types the surface-related rate constant k_{SA} is used as
397 general descriptor, for ZVI+AC systems this parameter varies with iron concentration (or in case
398 of Carbo-Iron with iron loading). Characterisation of the performance of ZVI+AC systems by
399 means of the observed rate constant k_{obs} is possibly more conclusive. A value of k_{obs} = 0.04 h^{-1}
400 for the mZVI+AC lies in the same order of magnitude is known for nanoscale ZVI as reductant.
401 This is especially remarkable since the mZVI sample applied is otherwise a very slow reductant.
402 However, it is common practice for ZVI users to compare iron performances on a per-mass or
403 per-surface basis. Therefore, k_{SA} values were also used here to evaluate the degradation of TCE
404 in the different systems as $k_{SA,ZVI-AC}/k_{SA,ZVI}$ formally. The experimental data in this study revealed
405 that bringing mZVI in contact with the AC felt FC 10 results in an immense improvement in
406 reaction rates, by three to four orders of magnitude ($k_{SA,mZVI/AC}/k_{SA,mZVI} \approx$ 1000 to 5000).
407 The obvious difference between the two dechlorination systems is the presumed reaction site.
408 At pristine mZVI, only the iron surface (more precisely its surface oxide layer) can act as
409 attachment and reaction site, whereas in the mZVI+AC system the dechlorination takes place at
410 the carbon surface, which offers a much higher surface area with a (tuneable) number of
411 reactive centres and probably also a different attachment mechanism than that at mZVI
412 surfaces. Almost 100 % of the educt TCE is in the adsorbed (reactive) state in the AC-containing

systems studied here, whereas >99 % are in the dissolved (nonreactive) state in pure mZVI suspensions.

3.3.3. Influence of surface modification of the AC sample FC 10 on the dechlorination rate

Table 2 and

Figure **3** indicate that the oxygen content and the type of surface functional groups determine the reaction rate and therefore the transfer of reduction equivalents towards the contaminants. Modification of the AC surface should provide more insight into the participation of functional groups in the dechlorination reaction. In this case, the degradation of PCE was examined. Wet oxidation of AC surfaces with nitric acid or hydrogen peroxide is often used to introduce oxygen-functional groups. The method using nitric acid was applied here in order to modify the AC felt FC 10 by wet oxidation. As described in the literature [48-50] and as revealed by the TPD analyses (Figure 7B), nitric acid caused not only a strong increase of acid groups, e.g. carboxylic or phenolic groups, but also a decrease of more thermally stable carbonyl groups, e.g. ketones or redox-active quinones [39]. In the batch experiment with the same amount of mZVI (not shown here), about a ten-fold lower dechlorination rate was found for PCE degradation than for the untreated AC felt. This conforms to our hypothesis that quinoid structures are essential by supporting the dechlorination in Fe+AC systems.

When AC is thermally treated above 1100 °C under inert atmosphere, most of the O-functional groups are split off as CO and CO_2. The thermal treatment in inert atmosphere (He) above 1100 °C was therefore used to modify the AC surface so as to remove the O-functional groups such that its dechlorination performance could be compared with untreated AC. The kinetics of

435 the PCE degradation (as formation of fully dechlorinated C_2-hydrocarbons) before and after the

436 modification are shown in Figure 6.

437

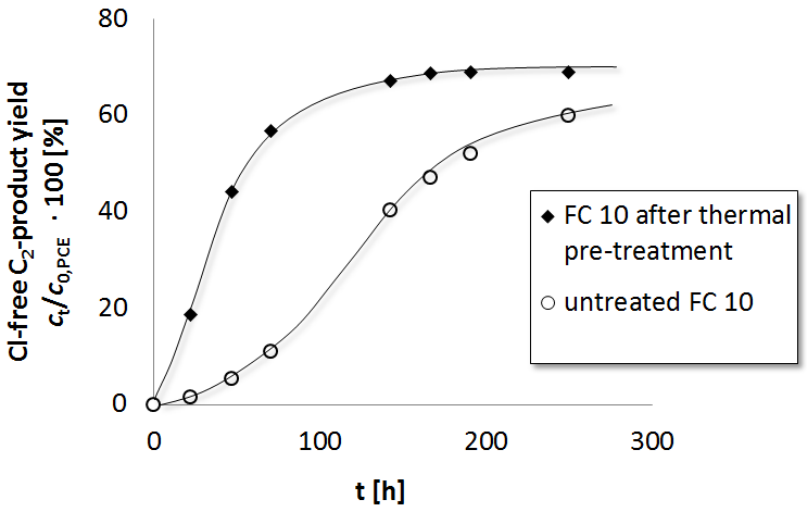

438

439 Figure 6: Kinetics of PCE degradation in the presence of mZVI and AC FC 10 before and after
440 thermal surface modification ($c_{0,PCE,total}$ = 25 mg L^{-1}, c_{FC10} = 1.8 g L^{-1}, c_{ZVI} = 20 g L^{-1},
441 c_{NaHCO3} = 5 mM, pH_{start} = 8.4).
442

443

444 Surprisingly, the heat-treated sample shows a high reactivity for PCE dechlorination and no
445 pronounced lag phase. This is the opposite of what we expected for an oxygen depleted carbon
446 surface. The TPD profile of the heat-treated FC 10 sample, shown in Figure 7C, reveals a CO peak
447 between 1000 and 1200 K. This can be tentatively assigned to relatively stable carbonyl or ether
448 groups, e.g. chromene or pyrone, which are formed when the AC is re-exposed to air after the
449 thermal treatment [35]. Since the modified carbon felt does not show the typical lag phase,
450 hydroquinones are not likely in this case as the redox mediator. Thus, other redox-active groups
451 may be involved. We hypothesize that pyrone and/or chromene groups at the AC surface can
452 also mediate the electron transfer from ZVI to chlorinated adsorbates [35,51].

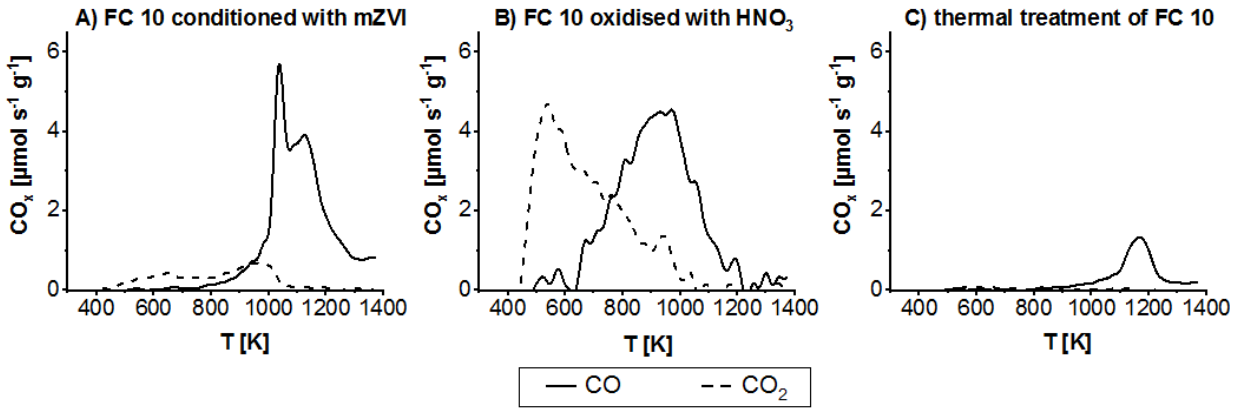

Figure 7: TPD profiles of the activated carbon FC 10 after various treatments (heating rate 10 K min^{-1}). A) 3 g L^{-1} FC 10 conditioned with 60 g L^{-1} mZVI for 5 days in aqueous environment, B) oxidised with HNO_3 and C) after thermal treatment and re-exposure to air.

3.3.4. Catalytic nature of AC activity

For an efficient utilization of the mZVI+AC system it is important to know whether the participating oxygen-containing functional groups of the AC felt can act catalytically or if they are irreversibly consumed. As shown above, it can be assumed that various surface groups are involved in the electron transfer process, whereby several observations in this study suggest that the quinone/hydroquinone redox couple plays a significant role for the unmodified felt FC 10. TPD analysis allows a semi-quantitative determination of these groups. The CO peak at about 1050 K can be assigned to phenolic species and was estimated to represent about 13 % of all CO-releasing groups (6.8 mmol g^{-1} AC) in the ZVI-treated sample (see Figure 7A). The participation of pyrones and chromenes plays a relatively minor role in the non-preteated felt, as TPD analysis and the typical lag phase at the beginning of the dechlorination run indicate. In order to test the catalytic activity of the AC felt FC 10, a typical batch experiment was

performed, with TCE added in excess compared to the concentration of the quinone/hydroquinone groups at the carbon surface (3.4 moles of TCE per mol of $OH_{hydroquinone}$, corresponding to 10.6 moles of e-acceptor per mol of e-donator). After about 170 and 350 h reaction time, the bottles were extensively purged with argon and spiked again with the same amount of TCE. The reaction progress was monitored via headspace analysis of the chlorine-free C_2-products and chloride analysis of the water phase, thus permitting the conclusion about the total TCE conversion. The results of the experiment are shown in Figure 9, where the derived turnover numbers (TON) over the monitoring period are depicted. The TON is calculated as the molar ratio of converted TCE, referred to the reactive hydroquinone centres (phenolic OH groups), taking into account a 4:1 stoichiometry. It was assumed that two molecules of hydroquinones (2 phenolic OH groups each) are necessary in order to convert one molecule of TCE into acetylene (see Figure 8). The degradation apparently followed zero-order kinetics with respect to TCE. Whereas during the first cycle a slightly higher conversion of TCE was observed within the monitoring time, it remained constant for the following two cycles. The slopes of the resulting graphs are similar for all three cycles. It is possible that oxygen-containing groups other than hydroquinones are also involved in the dechlorination reaction during the first cycle, whereby they are consumed during the reaction with TCE and not regenerated. The resulting overall TON was around 6 after 500 hours reaction time. This experiment proves the catalytic nature of the electron-transfer mediation by AC, rather than a stoichiometric consumption of AC reduction equivalents.

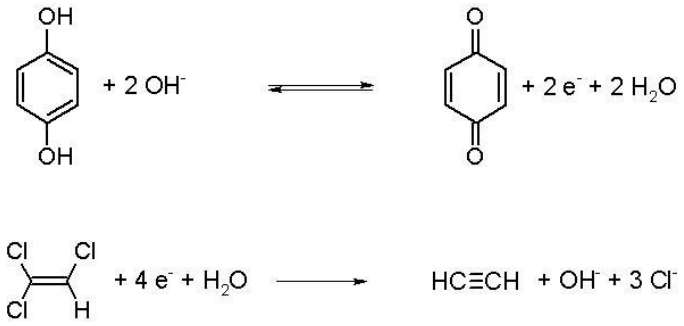

494

495 Figure 8: Assumed stoichiometry of the oxidation of hydroquinone and reduction of TCE
496
497

498

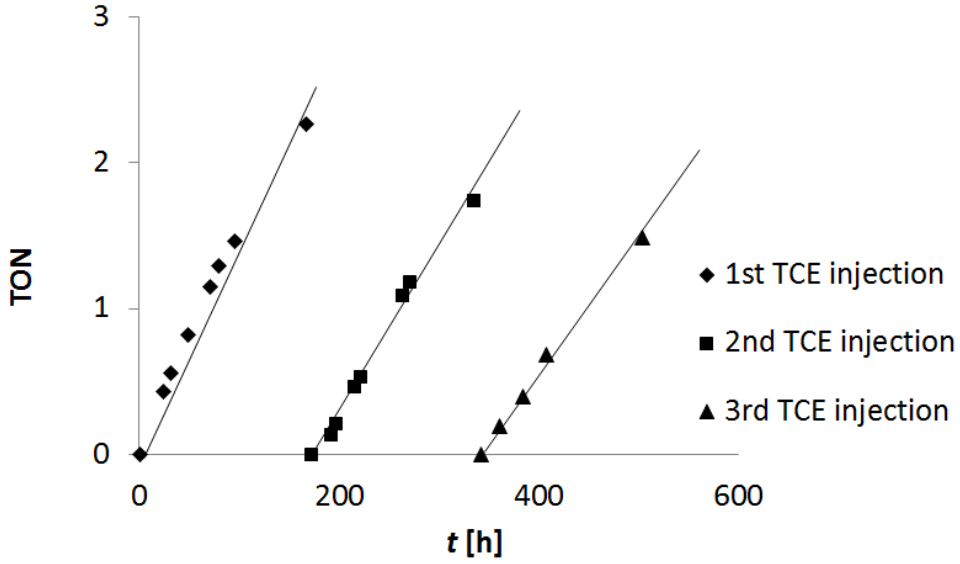

499

500 Figure 9: Turnover numbers (TON) of the TCE dechlorination in the mZVI/AC system
501 ($c_{0,TCE,total}$ = 1.6 g L^{-1}, c_{FC10} = 4.1 g L^{-1}, c_{ZVI} = 80 g L^{-1}, c_{NaHCO3} = 5 mM, pH_{start} = 8.4).
502
503

504 *3.3.5. Anaerobic corrosion of mZVI in the presence of the AC felt FC 10*

505 The anaerobic corrosion of ZVI is an undesired electron-consuming reaction competing with the
506 dechlorination reaction for the iron available. In addition, the ageing process of iron leads to
507 precipitations at the metal surface. During field application, even H_2 gas formation can lead to a
508 blockage of groundwater flow, thus by-passing the reaction zone. Dechlorination and anaerobic

corrosion often occur concurrently [52,53]. Most importantly, the corrosion rate determines the lifetime of ZVI in an aquifer, which is a crucial performance and cost parameter. This leads to the question of whether the high dechlorination activity of the mZVI+AC system is also accompanied by an increased anaerobic corrosion compared to the mZVI system. In order to elucidate the effect of AC contact for iron corrosion, the production of hydrogen gas was monitored at varying iron concentrations over a time period of 150 h and compared to the pure mZVI system. First-order rate constants $k_{H2,obs}$ (from $dc_{H2}/dt = k_{H2,obs} \cdot c_{mZVI}$) were calculated for the initial reaction phase and are presented in Figure 10**Fehler! Verweisquelle konnte nicht gefunden werden.**.

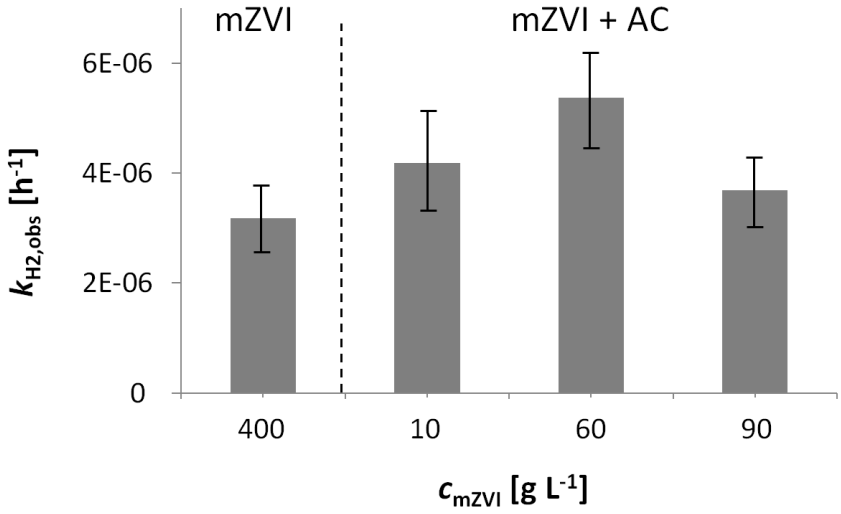

Figure 10: Anaerobic corrosion of mZVI alone and in the mZVI+AC system (c_{FC10} = 3.4 g L^{-1}, c_{NaHCO3} = 5 mM $NaHCO_3$, pH_{start} = 8.4). The error bar represents the mean deviation of single values from the mean value with n = 3.

In the mZVI+FC10 system, the anaerobic iron corrosion is with an average of $k_{H2,obs} = (4.4 \pm 0.9) \cdot 10^{-6}$ h^{-1} slightly higher than in the mZVI system with an average of $k_{H2,obs} = (3.2 \pm 0.6) \cdot 10^{-6}$ h^{-1}. However, both values are in the same range. It is likely that the ZVI+AC system acts as a local element to a small extent, as is known for cast-iron containing graphite [54].

Consequently, for the overall performance in the dechlorination of water pollutants, the combination of mZVI and AC textiles is favourable. The half-life of the investigated mZVI derived from the initial hydrogen formation rates amounts to about 23 years under the applied test conditions. As the corrosion is only increased to a minor extent by physical contact between ZVI and AC, the dechlorination efficiency (defined as ratio between dechlorination and corrosion rates) itself is markedly improved when ZVI is contacted with AC.

4. Conclusions and environmental implications

In the present paper, microiron contacting textile AC sheets (as one representative of AC) was inspected on a mechanistic basis using chlorinated ethenes as reaction probe. AC contact with otherwise barely reactive microiron can drastically accelerate the iron-based degradation of chlorinated ethenes by several orders of magnitude. The anaerobic corrosion of ZVI in the presence of AC is only slightly increased compared to the ZVI system, so that overall greatly increased dechlorination efficiency is achieved. The type of AC matters and determines the extent of rate acceleration. Especially the oxygen surface groups in AC, e.g., the

548 quinone/hydroquinone couple, were recognised as one of the main drivers for the redox-
549 mediating activity, whereby AC plays the role of a catalyst rather than a reactant. Iron “reloads”
550 the redox sites at the surface.
551 Consequently, the combination represents a method which is easy to apply and which helps to
552 better exploit the reduction capacity of metallic iron. We understand the manuscript as
553 supporting the possibility for end users to apply low-cost microiron or filings in order to reach
554 reactivities close to that of nanoiron, e.g. in on-site treatment plants. However, irrespective of
555 the application field, in-situ or on-site, a ZVI-based reaction zone can then be designed in such a
556 way that the residence time of the pollutant is sufficiently long to complete degradation. The
557 right choice of carbonaceous materials and its combination with ZVI largely increases the
558 retention time of organic contaminants compared with pure iron barriers / fixed beds. This
559 makes reactive zones or engineered reactors much smaller.
560

561 ## Acknowledgements

562 The authors thank the integrated project CCF at the Helmholtz Centre for Environmental
563 Research for financial support. Furthermore the authors are grateful for funding from the
564 research projects NanoREM (Project Nr.: 309517, EU 7th FP, NMP.2012.1.2) and Fe-Nanosit
565 (Project Nr.: BMBF 03X0082A). They also thank Maria Balda, Dr. Ulf Trommler and Navid Saeidi
566 for experimental support.
567

568 ## References

569 [1] F. Fu, D.D. Dionysiou, H. Liu, The use of zero-valent iron for groundwater remediation and
570 wastewater treatment: a review, J. Hazard. Mater. 267 (2014) 194–205.

[2] W. Yan, H.-L. Lien, B.E. Koel, W.-X. Zhang, Iron nanoparticles for environmental clean-up: Recent developments and future outlook, Environ. Sci. Process Impacts 15 (2013) 63–77.

[3] R.A. Crane, T.B. Scott, Nanoscale zero-valent iron: future prospects for an emerging water treatment technology, J. Hazard. Mater. 211-212 (2012) 112–125.

[4] R.M. Allen-King, R.M. Halket, D.R. Burris, Reductive transformation and sorption of cis- and trans-1,2-dichloroethene in a metallic iron-water system, Environ. Toxicol. Chem. 16 (1997) 424–429.

[5] D.R. Burris, T.J. Campbell, V.S. Manoranjan, Sorption of trichloroethylene and tetrachloroethylene in a batch reactive metallic iron-water system, Environ. Sci. Technol. 29 (1995) 2850–2855.

[6] D. Burris, R. Allen-King, V. Manoranjan, T. Campbell, G. Loraine, B. Deng, Chlorinated ethene reduction by cast iron: sorption and mass transfer, J. Environ. Eng. (1998) 1012–1019.

[7] J. Dries, L. Bastiaens, D. Springael, S.N. Agathos, L. Diels, Competition for sorption and degradation of chlorinated ethenes in batch zero-valent iron systems, Environ. Sci. Technol. 38 (2004) 2879–2884.

[8] M. Velimirovic, P.-O. Larsson, Q. Simons, L. Bastiaens, Impact of carbon, oxygen and sulfur content of microscale zerovalent iron particles on its reactivity towards chlorinated aliphatic hydrocarbons, Chemosphere 93 (2013) 2040–2045.

[9] W.-F. Chen, L. Pan, L.-F. Chen, Q. Wang, C.-C. Yan, Dechlorination of hexachlorobenzene by nano zero-valent iron/activated carbon composite: Iron loading, kinetics and pathway, RSC Adv. 4 (2014) 46689–46696.

[10] J. Gao, W. Wang, A.J. Rondinone, F. He, L. Liang, Degradation of trichloroethene with a novel ball milled Fe-C nanocomposite, J. Hazard. Mater. 300 (2015) 443–450.

[11] L. Han, S. Xue, S. Zhao, J. Yan, L. Qian, M. Chen, Biochar supported nanoscale iron particles for the efficient removal of methyl orange dye in aqueous solutions, PLOS One 10 (2015) e0132067.

[12] M. Lawrinenko, Z. Wang, R. Horton, D. Mendivelso-Perez, E.A. Smith, T.E. Webster, D.A. Laird, J.H. van Leeuwen, Macroporous carbon supported zerovalent iron for remediation of trichloroethylene, ACS Sustainable Chem. Eng. 5 (2017) 1586–1593.

[13] Z. Liu, F. Zhang, S.K. Hoekman, T. Liu, C. Gai, N. Peng, Homogeneously dispersed zerovalent iron nanoparticles supported on hydrochar-derived porous carbon: Simple, in Situ Synthesis and Use for Dechlorination of PCBs, ACS Sustainable Chem. Eng. 4 (2016) 3261–3267.

[14] K. Mackenzie, S. Bleyl, A. Georgi, F.-D. Kopinke, Carbo-Iron - An Fe/AC composite - As alternative to nano-iron for groundwater treatment, Water Res. 46 (2012) 3817–3826.

[15] X. Peng, X. Liu, Y. Zhou, B. Peng, L. Tang, L. Luo, B. Yao, Y. Deng, J. Tang, G. Zeng, New insights into the activity of a biochar supported nanoscale zerovalent iron composite and nanoscale zero valent iron under anaerobic or aerobic conditions, RSC Adv. 7 (2017) 8755–8761.

[16] Y.F. Su, Y.L. Cheng, Y.H. Shih, Removal of trichloroethylene by zerovalent iron/activated carbon derived from agricultural wastes, J. Environ. Manage. 129 (2013) 361–366.

[17] H.-H. Tseng, J.-G. Su, C. Liang, Synthesis of granular activated carbon/zero valent iron composites for simultaneous adsorption/dechlorination of trichloroethylene, J. Hazard. Mater. 192 (2011) 500–506.

[18] Y. Zhou, B. Gao, A.R. Zimmerman, H. Chen, M. Zhang, X. Cao, Biochar-supported zerovalent iron for removal of various contaminants from aqueous solutions, Bioresour. Technol. 152 (2014) 538–542.

[19] F.-D. Kopinke, G. Speichert, K. Mackenzie, E. Hey-Hawkins, Reductive dechlorination in water: Interplay of sorption and reactivity, Appl. Catal., B 181 (2016) 747–753.

[20] H. Tang, D. Zhu, T. Li, H. Kong, W. Chen, Reductive dechlorination of activated carbon-adsorbed trichloroethylene by zero-valent iron: carbon as electron shuttle, J. Environ. Qual. 40 (2011) 1878–1885.

[21] S.-Y. Oh, D.K. Cha, P.C. Chiu, Graphite-mediated reduction of 2,4-dinitrotoluene with elemental iron, Environ. Sci. Technol. 36 (2002) 2178–2184.

[22] F. Rodríguez-Reinoso, The role of carbon materials in heterogeneous catalysis, Carbon 36 (1998) 159–175.

[23] H.J. Amezquita-Garcia, E. Razo-Flores, F.J. Cervantes, J.R. Rangel-Mendez, Activated carbon fibers as redox mediators for the increased reduction of nitroaromatics, Carbon 55 (2013) 276–284.

[24] H. Fu, D. Zhu, Graphene oxide-facilitated reduction of nitrobenzene in sulfide-containing aqueous solutions, Environ. Sci. Technol. 47 (2013) 4204–4210.

[25] W. Xu, K.E. Dana, W.A. Mitch, Black carbon-mediated destruction of nitroglycerin and RDX by hydrogen sulfide, Environ. Sci. Technol. 44 (2010) 6409–6415.

[26] W. Xu, J.J. Pignatello, W.A. Mitch, Reduction of nitroaromatics sorbed to black carbon by direct reaction with sorbed sulfides, Environ. Sci. Technol. 49 (2015) 3419–3426.

[27] S.-Y. Oh, D.K. Cha, B.J. Kim, P.C. Chiu, Reduction of nitroglycerin with elemental iron - pathway, kinetics, and mechanisms, Environ. Sci. Technol. 38 (2004) 3723–3730.

[28] W. Chen, Y. Li, D. Zhu, S. Zheng, W. Chen, Dehydrochlorination of activated carbon-bound 1,1,2,2-tetrachloroethane: Implications for carbonaceous material-based soil/sediment remediation, Carbon 78 (2014) 578–588.

635 [29] K. Mackenzie, J. Battke, R. Koehler, F.-D. Kopinke, Catalytic effects of activated carbon on
636 hydrolysis reactions of chlorinated organic compounds, Appl. Catal., B 59 (2005) 171–179.
637 [30] K. Mackenzie, J. Battke, F.-D. Kopinke, Catalytic effects of activated carbon on hydrolysis reactions
638 of chlorinated organic compounds, Catal. Today 102-103 (2005) 148–153.
639 [31] L. Li, Q. Liu, Y.-X. Wang, H.-Q. Zhao, C.-S. He, H.-Y. Yang, L. Gong, Y. Mu, H.-Q. Yu, Facilitated
640 biological reduction of nitroaromatic compounds by reduced graphene oxide and the role of its
641 surface characteristics, Sci. Rep. 6 (2016) 30082.
642 [32] R.A. Pereira, M.F.R. Pereira, M.M. Alves, L. Pereira, Carbon based materials as novel redox
643 mediators for dye wastewater biodegradation, Appl. Catal., B 144 (2014) 713–720.
644 [33] Van der Zee, F., I.A.E. Bisschops, G. Lettinga, J.A. Field, Activated carbon as an electron acceptor
645 and redox mediator during the anaerobic biotransformation of azo dyes, Environ. Sci. Technol. 37
646 (2003) 402–408.
647 [34] B.M. Babic, S.K. Milonji, M.J. Polovina, B.V. Kaludierovi, Point of zero charge and intrinsic
648 equilibrium constants of activated carbon cloth, Carbon 37 (1999) 477–481.
649 [35] M.A. Montes-Morán, D. Suárez, J.A. Menéndez, E. Fuente, On the nature of basic sites on carbon
650 surfaces: An overview, Carbon 42 (2004) 1219–1225.
651 [36] S.M. Hassan, Reduction of halogenated hydrocarbons in aqueous media: I. Involvement of sulfur in
652 iron catalysis, Chemosphere 40 (2000) 1357–1363.
653 [37] Y. Sun, J. Li, T. Huang, X. Guan, The influences of iron characteristics, operating conditions and
654 solution chemistry on contaminants removal by zero-valent iron: A review, Water Res. 100 (2016)
655 277–295.
656 [38] M. Velimirovic, L. Carniato, Q. Simons, G. Schoups, P. Seuntjens, L. Bastiaens, Corrosion rate
657 estimations of microscale zerovalent iron particles via direct hydrogen production measurements,
658 J. Hazard. Mater. 270 (2014) 18–26.
659 [39] M.S. Shafeeyan, W.M.A.W. Daud, A. Houshmand, A. Shamiri, A review on surface modification of
660 activated carbon for carbon dioxide adsorption, J. Anal. Appl. Pyrolysis 89 (2010) 143–151.
661 [40] G.S. Szymański, Z. Karpiński, S.Biniak, A. Świątkowski, The effect of the gradual thermal
662 decomposition of surface oxygen species on the chemical and catalytic properties of oxidized
663 activated carbon. Carbon, 40 (2002) 2627-2639.
664 [41] A. Dandekar, R.T.K. Baker, M.A. Vannice, Characterization of activated carbon, graphitized carbon
665 fibers and synthetic diamond powder using TPD and DRIFTS. Carbon, 36 (1998) 1821-1831.
666 [42] J.L. Figueiredo, M.F.R. Pereira, M.M.A. Freitas, J.J.M. Orfao, Modification of the surface chemistry
667 of activated carbons. Carbon, 37 (1999) 1379-1389.[43] W.A. Arnold, A.L. Roberts, Pathways and

kinetics of chlorinated ethylene and chlorinated acetylene reaction with Fe(0) particles, Environ. Sci. Technol. 34 (2000) 1794–1805.

[44] D.S. He, C.P. Liu, Y.F. Yuan, X.Y. Li, Study on the adsorption of trichloroethylene in water on activated carbon and activated carbon fibers, Adv. Mat. Res. 113-116 (2010) 1021–1024.

[45] J. López, F. de La Cruz, Y. Alcaraz, F. Delgado, M.A. Vázquez, Quinoid systems in chemistry and pharmacology, Med. Chem. Res. 24 (2015) 3599–3620.

[46] A.E. Wendlandt, S.S. Stahl, Quinone-catalyzed selective oxidation of organic molecules, Angew. Chem. Int. Ed. Engl. 54 (2015) 14638–14658.

[47] L.H. Alvarez, I.C. Arvizu, R.B. García-Reyes, C.M. Martinez, D. Olivo-Alanis, Y.A. Del Angel, Quinone-functionalized activated carbon improves the reduction of congo red coupled to the removal of p-cresol in a UASB reactor, J. Hazard. Mater. 338 (2017) 233–240.

[48] J.L. Figueiredo, M.F.R. Pereira, M.M.A. Freitas, J.J.M. Órfão, Modification of the surface chemistry of activated carbons, Carbon 37 (1999) 1379–1389.

[49] J.L. Figueiredo, M.F.R. Pereira, M.M.A. Freitas, J.J.M. Órfão, Characterization of active sites on carbon catalysts, Ind. Eng. Chem. Res. 46 (2007) 4110–4115.

[50] J. Jaramillo, P.M. Álvarez, V. Gómez-Serrano, Oxidation of activated carbon by dry and wet methods, Fuel Process. Technol. 91 (2010) 1768–1775.

[51] E. Fuente, J.A. Menéndez, D. Suárez, M.A. Montes-Morán, Basic surface oxides on carbon materials: A Global View, Langmuir 19 (2003) 3505–3511.

[52] Y. Liu, S.A. Majetich, R.D. Tilton, D.S. Sholl, G.V. Lowry, TCE dechlorination rates, pathways, and efficiency of nanoscale iron particles with different properties, Environ. Sci. Technol. 39 (2005) 1338–1345.

[53] Y. Liu, G.V. Lowry, Effect of particle age (Fe0 content) and solution pH on nZVI reactivity: H2 Evolution and TCE Dechlorination, Environ. Sci. Technol. 40 (2006) 6085–6090.

[54] J.R. Davis, Corrosion: Understanding the basics, ASM International, Materials Park, Ohio, 2000.

[55] A.D. Henderson, A.H. Demond, Long-term performance of zero-valent iron permeable reactive barriers: A Critical Review, Environ. Eng. Sci. 24 (2007) 401–423.